A Simultaneous Cyber-attack and a Missile Attack

Bao U. Nguyen
Defence Research Development Canada, 101 Colonel By Drive, Ottawa, Canada
School of Mathematics and Statistics, University of Ottawa, 585 King Edward Avenue, Ottawa, Canada

Keywords: Cyber Defence, Missile Defence, Epidemic Models, Differential Equations, Probabilistic Models.

Abstract: We model a missile defence scenario where the red force infects the blue force command and control systems while at the same time launching re-entry vehicles toward the blue force. As a result, the blue force missile defence system is weakened due to loss of time, loss of engagement opportunities, loss of network centric capabilities etc. The impacts of the cyber-attack on missile defence metrics are determined through a number of key measures of effectiveness such as the probability of raid negation and the expected number of targets neutralized.

1 INTRODUCTION

In a traditional missile defence scenario, a number of re-entry vehicles (RVs) are launched toward a target. In response, the defence engages the threats with interceptors. Typically, such a scenario is analysed with the number of engagement opportunities and an engagement tactic to determine the metrics for missile defence such as the probability of raid annihilation, PRA, i.e. the probability of neutralizing all RVs.

With the advent of cyber technologies, the red force (the attacker) could also launch a cyber-attack at the same time as a missile attack or shortly before. This could lead the blue force (the defender) to lose precious time to counter the RVs, or to lose engagement opportunities, or to disable the defence net centric capabilities or to completely incapacitate the defence.

In this paper, we will model the cyber defence of the blue force through an epidemic model known as the SIR (Susceptible – Infected – Removed units) model (Smith?, 2008). There are of course other epidemic models e.g. Bailey, 1975, Hethcote, 2000 and Keeling and Rohani, 2007. However, we feel that the SIR model has a suitable level of details for this analysis. Morris-King and Cam, 2015 and Zou *et al.*, 2002 have also made use of epidemic models to investigate cyber vulnerabilities. The SIR model is described by three coupled differential equations. Among the simple epidemic models, this is the first that is not trivial and has no (elementary) known analytical solution. However, we were able to derive a relatively accurate analytical solution which is used to determine the time evolution of the SIR units. With this analytical solution, we estimate the impact of a cyber-attack on PRA and other metrics.

2 THE SIR MODEL

The premise of the SIR model is encoded in the following differential equations:

$$\begin{aligned} \frac{dS}{dt} &= -aSI \\ \frac{dI}{dt} &= aSI - bI \\ \frac{dR}{dt} &= bI \end{aligned} \tag{1}$$

where S is the number of susceptible units, I is the number of infected unit and R is the number of removed units i.e. the number of units that were infected and then recovered; a is the rate of infection and b is the rate of recovery.

Given that a missile attack lasts only a short time (approximately less than an hour), it is consistent with the SIR model that the population is a constant i.e. we assume that there is not sufficient time to add or remove new units. That is, $S + I + R = N$. Therefore, it is convenient to scale the SIR units so that the total population is one:

Nguyen, B.
A Simultaneous Cyber-attack and a Missile Attack.
DOI: 10.5220/0006847504930499
In *Proceedings of 8th International Conference on Simulation and Modeling Methodologies, Technologies and Applications (SIMULTECH 2018)*, pages 493-499
ISBN: 978-989-758-323-0
Copyright © 2018 by SCITEPRESS – Science and Technology Publications, Lda. All rights reserved

$$S'+I'+R'=N/N=1$$

where $S'=S/N$, $I'=I/N$, $R'=R/N$. For convenience, we refer to S' as S, I' as I and R' as R. Harko *et al.*, 2014 do provide a solution that is very sophisticated. Here, we favour a more simple approach that gives a simple solution.

Smith?, 2008 indicates that there are two equilibrium points. The first occurs when $I=\bar{I}=0$, $S=\bar{S}\le N$ and $R=\bar{R}=N-\bar{S}$ (the upper bar refers to the equilibrium values). This makes $dI/dt=0$. Hence, there is no infection. And the second occurs when $aS-b=0$ or $S=\bar{S}=b/a$ which also implies that $dI/dt=0$ which makes $I=\bar{I}\le N$ but S is decreasing due to dS/dt. Hence, this is not a stable equilibrium.

However, if $S_0>b/a$, the initial value of S at time zero will lead to an epidemic as the number of infected units I will increase with time at time zero since $dI/dt>0$.

Nguyen, 2017 shows that to solve the SIR model is equivalent to solve the following differential equation:

$$\frac{df}{dt}=1-bf-S_0e^{-af} \tag{2}$$

where

$$f(t)=\int_0^t I(t)\,dt\ge 0 \tag{3}$$

with boundary conditions:

$$\begin{aligned} f(0)&=\int_0^0 I(t)\,dt=0\\ \frac{df}{dt}&=I(0)=I_0\\ S(0)&=S_0\\ S_0+I_0&=1\\ R_0&=0 \end{aligned} \tag{4}$$

In addition, there are two roots (Mathematica 2011) to the RHS of Eqn (2):

$$\begin{aligned} f=f_1&=\frac{1}{b}+\frac{1}{a}W\left(-1,\frac{-aS_0}{b}e^{-a/b}\right)\\ f=f_2&=\frac{1}{b}+\frac{1}{a}W\left(0,\frac{-aS_0}{b}e^{-a/b}\right) \end{aligned} \tag{5}$$

with W the Lambert functions. For a real argument x, there are two branches to the Lambert functions: $W(-1,x)$ and $W(0,x)$, Mathematica, 2011. Based on the characteristics of the Lambert function, Nguyen, 2017 shows that $f_2\ge 0$ and $f_1\le 0$. Nguyen, 2017 also shows that the RHS of Eqn (2) is a convex function in f. This leads to an approximation of the RHS of Eqn (2) as a quadratic function:

$$1-bf-e^{-af}\sim c(f-f_1)(f-f_2) \tag{6}$$

While Eqn (6) captures the convexity of Eqn (2), Eqn (6) does not reproduce the asymmetry of Eqn (2). This is so as a quadratic function in f is a symmetrical function with respect to its vertex $\left(f=(f_1+f_2)/2\right)$. Therefore, we propose an improvement to this approximation.

3 NEW APPROXIMATION TO THE SIR MODEL

As a correction to Eqn (6), we introduce a parameter δ such that

$$1-bf-e^{-af}\sim c(f-f_1)^{1-\delta}(f_2-f)^{1+\delta} \tag{7}$$

δ is chosen so that the LHS and the RHS of Eqn (7) match at $f=f^*=\dfrac{\ln(a\cdot S_0/b)}{a}$ where the LHS of Eqn (7) is a maximum.

Since the LHS of Eqn (7) is a convex function, this is the only maximum. Hence, there is no ambiguity in determining δ:

$$\delta=\frac{f^*/2-(f_1+f_2)}{f_1-f_2} \tag{8}$$

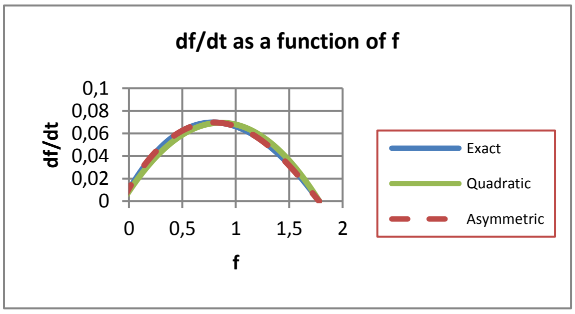

Figure 1: df/dt from Eqn (2), quadratic approximation in Eqn (6) and asymmetric approximation Eqn (7) – ($a=1/2$, $b=1/3$, $S_0=0.99$, $I_0=0.01$ and $R_0=0$).

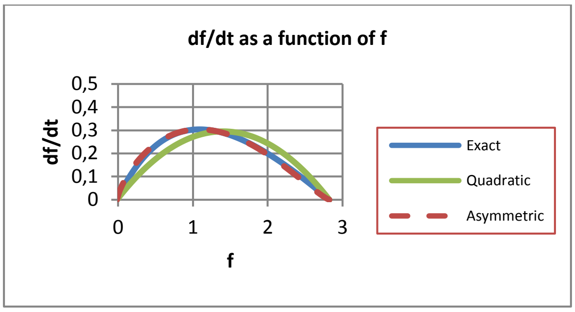

Figure 2: df/dt from Eqn (2), quadratic approximation in Eqn (6) and asymmetric approximation Eqn (7) – ($a=3/2$, $b=1/3$, $S_0=0.99$, $I_0=0.01$ and $R_0=0$).

Figure 1 shows df/dt as a function of f for three cases: the exact case, the quadratic approximation and the asymmetric approximation. We assume that $a=1/2$, $b=1/3$, $S_0=0.99$, $I_0=0.01$ and $R_0=0$. It can be seen that the three cases are similar.

Figure 2 also shows df/dt as a function of f for three cases: the exact case, the quadratic approximation and the asymmetric approximation. We assume that $a=3/2$, $b=1/3$, $S_0=0.99$, $I_0=0.01$ and $R_0=0$. It can be seen that the quadratic approximation is distinct from the two other cases.

Note that the values of the above parameters -- a, b, S_0, I_0 and R_0 -- were used for illustration purposes only.

Using the approximation on the RHS of Eqn (7), i.e.

$$\frac{df}{dt}=c\left(f-f_1\right)^{1-\delta}\left(f_2-f\right)^{1+\delta} \tag{9}$$

or

$$\frac{df}{c\left(f-f_1\right)^{1-\delta}\left(f_2-f\right)^{1+\delta}}=dt$$

We obtain:

$$\frac{1}{c}\cdot\frac{\left(f-f_1\right)^{\delta}\cdot\left(f_2-f\right)^{-\delta}}{\delta\cdot\left(f_2-f_1\right)}=t+A$$

Since $f=0$ when $t=0$, we get:

$$A=\frac{1}{c}\cdot\left(\frac{-f_1}{f_2}\right)^{\delta}\cdot\frac{1}{\delta\cdot\left(f_2-f_1\right)} \tag{10}$$

Matching Eqn (7) at $f=f^*$ dictates that:

$$c=\frac{1-b/a\cdot\left(1+\ln\left(a\cdot S_0/b\right)\right)}{\left(f^*-f_1\right)^{1-\delta}\cdot\left(f_2-f^*\right)^{1+\delta}} \tag{11}$$

Now that all of the parameters are well defined, we could solve Eqn (9):

$$f=f_2-\frac{f_2-f_1}{1+u} \tag{12}$$

where

$$u=\left[c\cdot\delta\cdot\left(f_2-f_1\right)\cdot\left(t+A\right)\right]^{1/\delta} \tag{13}$$

Since $I=df/dt$, we get:

$$I=\frac{c\cdot\left(f_2-f_1\right)^2\cdot u^{1-\delta}}{\left(1+u\right)^2} \tag{14}$$

By manipulating Eqn (1), Nguyen, 2017 shows that:

$$S=S_0\cdot e^{-a\cdot f(t)} \tag{15}$$

and

$$R=b\cdot f\left(t\right) \tag{16}$$

4 PROPERTIES OF THE APPROXIMATION

The maximum of I occurs when $dI/dt=0$. Using Eqn (14), we get:

$$I_{\max}=c\cdot\left(f_2-f_1\right)^2\cdot\frac{\left(u^*\right)^{1-\delta}}{\left(1+u^*\right)^2} \tag{17}$$

where

$$u^*=\frac{1-\delta}{1+\delta} \tag{18}$$

This corresponds to

SCITEPRESS SCIENCE AND TECHNOLOGY PUBLICATIONS

$$t^* = \frac{\left(u^*\right)^{\delta}}{c \cdot \delta} - A \tag{19}$$

Taking the limit as $t \to \infty$ of Eqn (14) yields:

$$\lim_{t \to \infty} I = 0 \tag{20}$$

Similarly,

$$\lim_{t \to \infty} f = f_2 \tag{21}$$

Therefore,

$$\lim_{t \to \infty} S = S_0 \cdot e^{-a \cdot f_2} \tag{22}$$

and

$$\lim_{t \to \infty} R = b \cdot f_2 \tag{23}$$

Note that by taking the limit $\delta \to 0$, we recover the results of Nguyen 2017 i.e.

$$\lim_{\delta \to 0} u = \left(\frac{-f_1}{f_2}\right) \cdot e^{c \cdot (f_2 - f_1) \cdot t} \tag{24}$$

We display below S, I and R as a function of time. The exact case is obtained numerically using Mathematica, 2011.

Note that we could also determine the time when I decreases to a small amount ε after it reaches the maximum value. That is,

$$I = \frac{c \cdot \left(f_2 - f_1\right)^2 \cdot u^{1-\delta}}{\left(1+u\right)^2} = \varepsilon \tag{25}$$

or

$$u^{1-\delta} = \varepsilon' \cdot \left(1+u\right)^2 \tag{26}$$

where

$$\varepsilon' = \frac{\varepsilon}{c \cdot \left(f_2 - f_1\right)^2} \tag{27}$$

We use perturbation theory to get the first order approximation for $u = u_0 + \delta \cdot u_1 + O\left(\delta^2\right)$ by expanding Eqn (26) as a series in powers of δ. By carefully the value of u that occurs after the maximum of I, we get:

$$u_0 = \frac{1 - 2 \cdot \varepsilon' + \sqrt{1 - 4 \cdot \varepsilon'}}{2 \cdot \varepsilon'} = \frac{1}{\varepsilon'} - 2 + O\left(\varepsilon'\right) \tag{28}$$

and

$$u_0 = \frac{1 - 2 \cdot \varepsilon' + \sqrt{1 - 4 \cdot \varepsilon'}}{2 \cdot \varepsilon'} = \frac{1}{\varepsilon'} - 2 + O\left(\varepsilon'\right) \tag{29}$$

$$u_1 = \frac{u_0 \cdot \ln\left(u_0\right)}{1 - 2 \cdot \varepsilon' \cdot \left(1 + u_0\right)} = \frac{\ln\left(\varepsilon'\right)}{\varepsilon'} + 2 + O\left(\varepsilon'\right) \tag{30}$$

Hence,

$$t = \frac{\left(u_0 + \delta \cdot u_1 + O\left(\delta^2\right)\right)^{\delta}}{c \cdot \delta} - A \tag{31}$$

This works for very small values of δ and very small values of ε'. An alternative, accurate and efficient way to determine the time is to use the rigorous bisection methodology in Press et al. 1992 where would be bracketed in the interval:

$$\left[\frac{1}{\sqrt{\varepsilon'}} - 1, u_0\right] \tag{32}$$

The corresponding time can be determined in a similar way to Eqn (19) (without the $*$).

Figures 3, 4 and 5 show that the approximations reproduce the characteristics of the exact numerical solution. S decreases monotonically as a function of time. I increases and then decreases as a function of time. R increases monotonically as a function of time. The asymmetric approximation is clearly closer to the exact solution than the quadratic approximation. More importantly, the asymmetric approximation replicates the asymmetry of df/dt which is essential to the SIR model since there is no reason for the independent parameters a and b to combine in a way such that df/dt is symmetric in f.

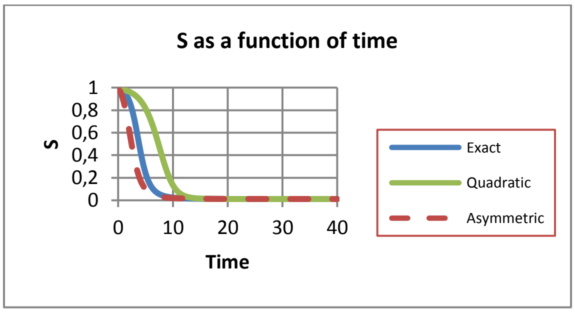

Figure 3: S as a function of time for the exact case, the quadratic approximation and the asymmetric approximation.

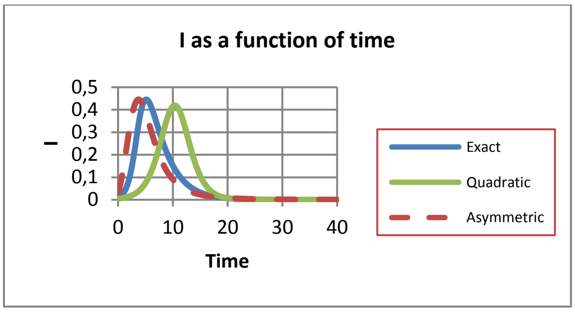

Figure 4: I as a function of time for the exact case, the quadratic approximation and the asymmetric approximation.

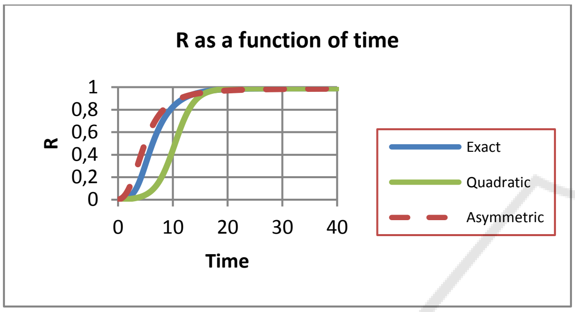

Figure 5: R as a function of time for the exact case, the quadratic approximation and the asymmetric approximation.

5 EFFECTS ON MISSILE DEFENCE

To examine the impacts of infection on missile defence capabilities, we consider a scenario where there are three re-entry vehicles (RVs) and six interceptors. We assume that there are two engagement opportunities.

Normally, given the speeds and ranges involved Cranford, 2004 could be used to determine the number of engagement opportunities for ballistic missile trajectories. The key metrics are the probability of raid annihilation (PRA) -- the probability of neutralizing all RVs, the expected number of RVs neutralized $(ERVN)$ and the expected number of interceptors expended $(ENIE)$. These metrics are parametrized by the single shot probability of a hit H.

When the defence is infected with viruses, the missile defence capabilities could also be affected. As shown in Figure 4, it takes the defence about twenty minutes to remove the infection. We consider below three possible scenarios:

A. The defence is unaffected;
B. The defence loses one engagement opportunity and
C. The defence loses its coordination such as its network centric capabilities.

In scenario A, the defence uses a shoot-look-shoot tactic. It engages each RV with one interceptor at each engagement opportunity. If the RV is neutralized then the defence will stop engaging that RV. Otherwise, the defence will re-engage the RV with another interceptor until the defence runs out of interceptors or engagement opportunities. The metrics for scenario A are given below.

$$PRA = \left(1 - M^2\right)^3 \tag{33}$$

$$ERVN = 3 \cdot \left(1 - M^2\right) \tag{34}$$

$$ENIE = 3 + 3 \cdot M \tag{35}$$

where $M = 1 - H$.

In scenario B, the defence will launch all of its interceptors at the second engagement opportunity. This gives:

$$PRA = \left(1 - M^2\right)^3 \tag{36}$$

$$ERVN = 3 \cdot \left(1 - M^2\right) \tag{37}$$

$$ENIE = 6 \tag{38}$$

In scenario C, the defence loses its coordination hence it cannot allocate the interceptors optimally among the RVs. The optimal allocation occurs when the defence assigns the interceptors as evenly as possible among the RVs, Soland, 1987, at each engagement opportunity. The possible allocations are determined in Nguyen and Miah, 2015 as shown in Table 1.

Table 1: All possible engagement allocations against three RVs.

Engagement allocation	RV 1	RV 2	RV 3
1	0	0	6
2	0	1	5
3	0	2	4
4	0	3	3
5	1	1	4
6	1	2	3
7 (Optimal Salvo tactic)	2	2	2

Assuming that each allocation in Table 1 is equally probable then PRA can be expressed as:

$$PRA = \frac{1}{7} \cdot \sum_{i=1}^{7} p_i \tag{39}$$

where

$$p_1, p_2, p_3, p_4 = 0 \tag{40}$$

$$p_5 = (1-M)^2 \cdot (1-M^4) \tag{41}$$

$$p_6 = (1-M) \cdot (1-M^2) \cdot (1-M^3) \tag{42}$$

$$p_7 = (1-M^2)^3 \tag{43}$$

As well, $ERVN$ can be expressed as:

$$ERVN = \frac{1}{7} \cdot \sum_{i=1}^{7} e_i \tag{44}$$

$$e_1 = 1 - M^6 \tag{45}$$

$$e_2 = 2 - M - M^5 \tag{46}$$

$$e_3 = 2 - M^2 - M^4 \tag{47}$$

$$e_4 = 2 - 2 \cdot M^3 \tag{48}$$

$$e_5 = 3 - 2 \cdot M - M^4 \tag{49}$$

$$e_6 = 3 - M - M^2 - M^3 \tag{50}$$

$$e_7 = 3 - 3 \cdot M^2 \tag{51}$$

Also, $ENIE$ is given by:

$$ENIE = 6 \tag{52}$$

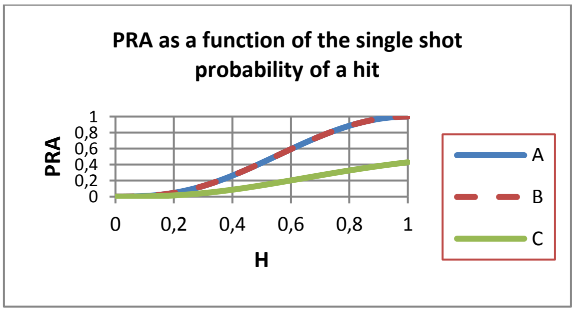

Figure 6: PRA as a function of the single shot probability of a hit H.

Figures 6, 7 and 8 plot the missile defence metrics as a function of the single shot probability of a hit H. It is seen that PRA and $ERVN$ are the same for scenario A and for scenario B. However,

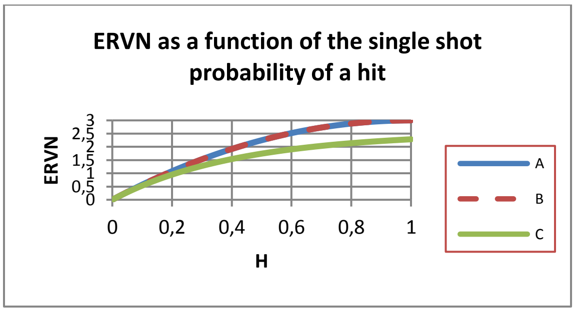

Figure 7: $ERVN$ as a function of the single shot probability of a hit H.

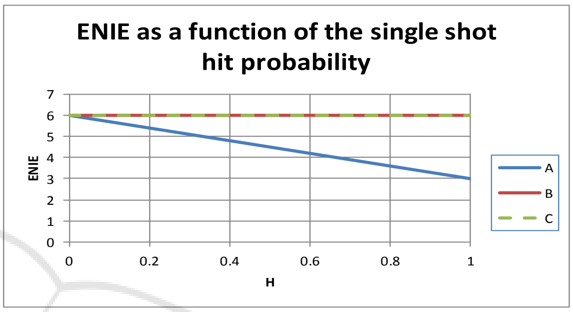

Figure 8: $ENIE$ as a function of the single shot probability of a hit H.

they are substantially lower for scenario C. This is due to the fact that in scenario C, the engagement allocation is not optimal.

$ENIE$ is equal to six for scenario B and scenario C but is decreasing as a function of H for scenario A. This means that in scenario B and in scenario C, the defence launches all of its interceptors. This is very dangerous as the defence will not have any interceptors left to engage unexpected RVs or to re-engage RVs that were missed due to malfunctions of the defence systems. For scenario A, with a typical H of seventy percent, Figure 8 shows that the defence will have expended four interceptors implying the defence will have two interceptors remaining for unexpected events. As H increases, $ENIE$ decreases and so the number of interceptors saved increases.

We observe that when the number of RVs and the number of interceptors are large, the metrics such as PRA and $ERVN$ can be efficiently determined using a generating function e.g. Nguyen *et al.*, 1997. Missile defence can also be modelled using Markov chains e.g. Menq *et al.*, 2007 and globally optimized using dynamic programming e.g. Soland, 1987.

SCITEPRESS SCIENCE AND TECHNOLOGY PUBLICATIONS

6 CONCLUSIONS

In this paper, we examine a missile attack scenario combined with a cyber-attack scenario. To do that, we solve the SIR model using an approximate solution which reproduces all of the characteristics of the problem such as the asymmetry, the trends in time evolution of the parameters I , S and R as well as their long term behaviours.

It could also be argued that the asymmetric approximation is in itself an epidemic model in the same way that the SIR model is an epidemic model. They are both anchored on similar assumptions. And they both generate similar results.

We show that the missile defence effectiveness of the blue force can be critically affected when the red force launches a cyber-attack at the same time as a missile attack.

To our knowledge, the degradations of a missile defence system due to a cyber-attack have not been explicitly modelled. In the future, we would like to examine closely how command and control systems are affected by a cyber-attack. To do that, we will investigate in depth the complexity of command and control systems and the nature of cyber-attacks.

REFERENCES

Bailey, N.T.J., 1975. *The mathematical theory of infectious diseases and its applications*, Charles Griffin and Company LTD, 2nd edition, pp. 39-42.

Cranford K.. 2004. *Battle Area Region Threatened Model (BART).* NORAD-USNORTHCOM/AN (North American Aerospace Defense Command – United States Northern Command/Center for Aerospace Analysis) Version 5.3.4x. and the CheckThreats subroutine.

Harko, T., Lobo, F.S.N., and Mak, M.K., 2014. 'Exact analytical solutions of the Susceptible-Infected-Recovered (SIR) epidemic model and of the SIR model with equal death and birth rates', *Applied Mathematics and Computation*, 236, pp. 184-194.

Hethcote, H., 2000. 'The mathematics of infectious diseases', SIAM Review, Vol. 42, No. 4, pp. 599-653.

Keeling, M.J. and Rohani, P., 2007. *Modeling Infectious Diseases in Humans and Animals,* Princeton University Press, p. 4.

Mathematica 2011. Wolfram Research Inc.

Menq J.-Y., Tuan P.-C. and Liu T.-S., 2007. 'Discrete Markov Ballistic Missile Defense System Modeling', *European Journal of Operational Research*, 178, pp. 560–578.

Morris-King, J. and Cam, H., 2015. 'Ecology-inspired cyber risk model for propagation of vulnerability exploitation in tactical edge', *Proceedings of the IEEE 2015 Military Communications Conference MILCOM'2015*, pp. 336-341.

Nguyen B.U., Smith P.A. and Nguyen D., 1997. 'An Engagement Model to Optimize Defense Against a Multiple Attack Assuming Perfect Kill Assessment', *Naval Research Logistics*, 44, pp. 687-697.

Nguyen, B.U., 2017. 'Modelling cyber vulnerabilities using epidemic models', *7th international conference on simulation and modelling methodologies, technologies and applications*.

Nguyen, B. and Miah, S., 2015. '*Comparison of metrics for missile defence between perfect coordination and no coordination*', DRDC Scientific Report (SR) DRDC-RDDC-2015-R228.

Press, W.H., Flannery, B.P., Teukolsky, S.A. and Vetterling W.T., 1992. *Numerical recipes in Fortran 77 (The Art of Scientific Computing).* Cambridge University Press, 2nd edition, pp. 343-347.

Smith? R., 2008. *Modelling disease ecology with mathematics*, American Institute of Mathematical Sciences, pp. 14-30.

Soland, R. M., 1987. 'Optimal Terminal Defense Tactics when Several Sequential Engagements Are Possible', *Operations Research*, 35, pp. 537-542.

Zou, C.C., Gong, W., and Towsley, D., 2002. Code red worm propagation modeling and analysis, *Proceedings of the 9th ACM conference on Computer and communications security*, pp. 138-147.